Inorg. Chem. **1989**, *28*, 2103–2106

Contribution from the Institute of Chemistry, Academia Sinica,
and Department of Chemistry, National Taiwan University, Taipei, Taiwan, ROC

Electron Transfer in the Mixed-Valence Complexes (*E*)- and (*Z*)-1,2-Bis(1′-ethyl-1-ferrocenyl)-1,2-dimethylethylene

Teng-Yuan Dong,*[,1] Tze-Juine Ke, Shie-Ming Peng,*[,2] and Show-Kei Yeh

Received July 15, 1988

The physical properties of neutral and mixed-valence (*E*)- and (*Z*)-1,2-bis(1′-ethyl-1-ferrocenyl)-1,2-dimethylethylene are reported. The structure of the *E* isomer has been determined by using the heavy-atom method and a four-circle X-ray diffractometer. The compound crystallizes with triclinic symmetry, space group $P\bar{1}$, $a = 7.507$ (4) Å, $b = 10.837$ (4) Å, $c = 13.871$ (3) Å, $\alpha = 93.191$ (25)°, $\beta = 96.70$ (3)°, $\gamma = 90.18$ (4)°, $V = 1122.66$ Å^3, and $Z = 2$. The structure was refined to give conventional discrepancy factors of $R_F = 0.053$ and $R_{wF} = 0.062$. The surprisingly similar physical properties for the *E* and *Z* ethylene-bridged mixed-valence complexes, especially in comparison with the electrochemical measurements and the absorption profile for the intervalence band, indicate that intramolecular electron transfer in these species is associated with *E–Z* and *Z–E* isomerizations.

Introduction

There is growing interest in studying electron transfer for mixed-valence transition-metal complexes.[3] The study of mixed-valence compounds will potentially aid in understanding what factors[4] control the rate of electron transfer as found in oxidation–reduction, electrochemical, and biological processes.[5]

In very recent studies it has been shown that the solid-state environment plays a crucial role in determining the rate of intramolecular electron transfer in various mixed-valence biferrocenium salts.[6] Four 1′,1‴-dialkylbiferrocenium triiodides (X = $-CH_2CH_3$, $-CH_2CH_2CH_3$, $-CH_2CH_2CH_2CH_3$, $-CH_2C_6H_5$) make an interesting series.

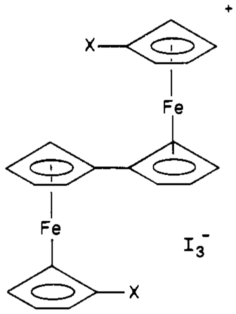

1a: X = H
b: X = C_2H_5
c: X = C_3H_7
d: X = C_4H_9
e: X = $CH_2C_6H_5$

The four complexes give unusual temperature-dependent Mössbauer spectra. In previous papers, we suggested that it is the environment about the mixed-valence cation in the solid state that controls whether and at what temperature intramolecular electron transfer occurs.[7]

In an extension of our studies on intramolecular electron transfer in the mixed-valence biferrocenium cation, complexes **2** and **3** were prepared. The bridged complexes **2** and **3** provide the opportunity to study intramolecular electron transfer between electron donor and electron acceptor as a function of the relative orientation and separation of donor and acceptor. The nature and extent of dependence of rates of electron transfer on distance between donor and acceptor sites have been a central concern of electron-transfer dynamics.[8] Various naturally occurring proteins and unsaturated and saturated organic bridges have been employed in the distance-dependence studies.[3] The focus of this paper is electron transfer in the presence of a complicating conformational effect.

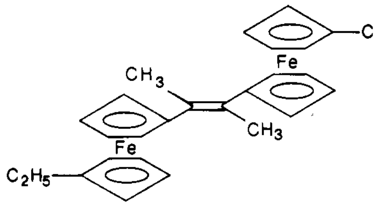

2

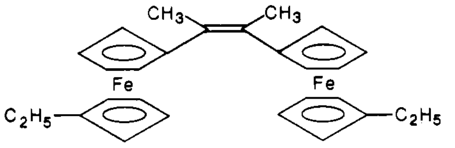

3

Experimental Section

Compound Preparation. Samples of 1-ethyl-1′-acetylferrocene[9] and biferrocene[10] were prepared according to literature methods and identified by melting point, NMR, and mass spectral data. Solvents were routinely dried by standard procedures and stored under nitrogen.

Reductive Coupling of 1-Ethyl-1′-acetylferrocene. To a solution of $TiCl_4$ (50 mmol) in dry THF (50 mL) cooled in an ice–salt bath was added $LiAlH_4$ (26 mmol). The mixture was refluxed for 1 h under a nitrogen atmosphere to give a deep black solution. To this black solution was added dropwise a solution of 1-ethyl-1′-acetylferrocene (10 mmol) and tributylamine (10 mmol) in dry THF (20 mL) for 5 h under reflux conditions. The mixture was quenched with 20% K_2CO_3 aqueous solution. After filtration, the filtrate was extracted with CH_2Cl_2. The combined CH_2Cl_2 extracts were washed with H_2O and dried over $MgSO_4$, and the solvent was removed on a rotary evaporator. These crude products were chromatographed on neutral alumina (activity I) with hexane to give a mixture of **2** and **3**. The *E* and *Z* isomers were separated by several fractional recrystallizations in hexane at −40 and −78 °C, respectively. The yields for **2** and **3** are 32% and 14%, respectively. The properties of the *E* isomer (**2**) are as follows: mp 93.5–94 °C; ^1H NMR ($CDCl_3$) δ 1.186 (t, 6 H, $-CH_3$), 2.167 (s, 5.8 H, $=CCH_3$), 2.333 (q, 3.8 H, $-CH_2$), 4.057 (s, 8 H, Cp $H_{\alpha,\beta}$), 4.173 (d, 4 H, Cp H_β), 4.262 (d, 4 H, Cp H_α); electron-impact mass spectrum M^+ at m/e 480. The properties of the *Z* isomer (**3**) are as follows: mp 51–52 °C; ^1H NMR

---

(1) Academia Sinica.

(2) National Taiwan University.

(3) (a) Day, P. *Int. Rev. Phys. Chem.* **1981**, *1*, 149. (b) Brown, D. B., Ed. *Mixed-Valence Compounds, Theory and Applications in Chemistry, Physics, Geology and Biology*; Reidel: Boston, MA, 1980. (c) Creutz, C. *Prog. Inorg. Chem.* **1983**, *30*, 1. (d) Richardson, D. E.; Taube, H. *Coord. Chem. Rev.* **1984**, *60*, 107.

(4) Wong, K. Y.; Schatz, P. N. *Prog. Inorg. Chem.* **1981**, *28*, 369 and references therein.

(5) (a) Devault, D., Ed. *Quantum-Mechanical Tunnelling in Biological Systems*, 2nd ed.; Cambridge University: Cambridge, England, 1984. (b) Cannon, R. D., Ed. *Electron Transfer Reactions*; Butterworths: Boston, MA, 1980. (c) Marcus, R. A.; Sutin, N. *Biochim. Biophys. Acta* **1985**, *811*, 265.

(6) (a) Cohn, M. J.; Dong, T.-Y.; Hendrickson, D. N.; Geib, S. J.; Rheingold, A. L. *J. Chem. Soc., Chem. Commun.* **1985**, 1095. (b) Dong, T.-Y.; Kambara, T.; Hendrickson, D. N. *J. Am. Chem. Soc.* **1986**, *108*, 4423. (c) Dong, T.-Y.; Hendrickson, D. N.; Iwai, K.; Cohn, M. J.; Geib, S. J.; Reingold, A. L.; Sano, H.; Motoyama, I.; Nakashima, S. *J. Am. Chem. Soc.* **1985**, *107*, 7996.

(7) (a) Kambara, T.; Hendrickson, D. N.; Dong, T.-Y.; Cohn, M. J. *J. Chem. Phys.* **1987**, *86*, 2362. (b) Sorai, M.; Nishimori, A.; Hendrickson, D. N.; Dong, T.-Y.; Cohn, M. J. *J. Am. Chem. Soc.* **1987**, *109*, 4266.

(8) Hush, N. S. *Coord. Chem. Rev.* **1985**, *64*, 135.

(9) Nesmeyanov, A. N.; Spulpin, G. B.; Rybinskaya, M. I. *Izv. Akad. Nauk SSSR, Ser. Khim.* **1975**, 2824.

(10) Rausch, M. D. *J. Org. Chem.* **1961**, *26*, 1802.

0020-1669/89/1328-2103$01.50/0

Table I. Analytical Data

compd	% calcd			% found		
	C	H	I	C	H	I
(*Z*)-1,2-dimethyl-1,2-ethenediylbis(1′-ethylferrocenium) triiodide	27.08	2.60	61.32	27.16	2.48	60.88
(*E*)-1,2-dimethyl-1,2-ethenediylbis(1′-ethylferrocenium) triiodide	27.08	2.60	61.32	27.43	2.52	61.20
biferrocenium triiodide	32.00	2.42	50.71	32.15	2.38	50.92

Table II. Crystallographic Data for **2**

chem formula: $C_{28}H_{32}Fe_2$	fw: 480.258
a = 7.507 (4) Å	space group: $P\bar{1}$
b = 10.873 (4) Å	T = 25.0 °C
c = 13.871 (3) Å	λ = 0.7101 Å
α = 93.191 (25)°	ρ_{calcd} = 1.421 g cm^{-3}
β = 96.70 (3)°	μ = 1.33 mm^{-1}
γ = 90.18 (4)°	$R_F{}^a$ = 0.053
V = 1122.66 Å^3	$R_{wF}{}^a$ = 0.063
Z = 2	

[a] $R_F = \sum|F_o - |F_c||/\sum F_o$; $R_{wF} = [\sum w(F_o - |F_c|)^2/\sum wF_o{}^2]^{1/2}$.

Table III. Atom Coordinates and Thermal Parameters for **2**

atom	x	y	z	U_{iso},[a] Å^2
Fe(1A)	0.12189 (6)	0.55490 (4)	0.30810 (4)	2.880 (22)
Fe(1B)	0.61738 (6)	0.06239 (4)	0.25302 (3)	2.834 (21)
C(1A)	0.4921 (5)	0.6762 (3)	0.4777 (3)	3.40 (15)
C(2A)	0.4656 (4)	0.5383 (3)	0.46624 (24)	2.66 (14)
C(3A)	0.3656 (4)	0.4941 (3)	0.3722 (3)	2.80 (14)
C(4A)	0.2378 (4)	0.3953 (3)	0.3509 (3)	3.15 (15)
C(5A)	0.1811 (5)	0.3866 (3)	0.2506 (3)	3.69 (15)
C(6A)	0.2698 (5)	0.4805 (3)	0.2063 (3)	3.74 (16)
C(7A)	0.3822 (5)	0.5473 (3)	0.2821 (3)	3.17 (14)
C(8A)	−0.0956 (10)	0.6612 (8)	0.0620 (6)	10.2 (5)
C(9A)	−0.0323 (9)	0.7413 (6)	0.1445 (5)	8.5 (3)
C(10A)	−0.0402 (6)	0.6832 (4)	0.2416 (4)	5.11 (21)
C(11A)	−0.1450 (5)	0.5842 (4)	0.2682 (4)	5.12 (21)
C(12A)	−0.1106 (6)	0.5744 (4)	0.3695 (4)	5.44 (24)
C(13A)	0.0139 (6)	0.6698 (5)	0.4058 (3)	5.22 (21)
C(14A)	0.0527 (6)	0.7350 (4)	0.3267 (4)	5.18 (22)
C(1B)	0.7572 (4)	−0.0317 (3)	0.4973 (3)	3.22 (14)
C(2B)	0.5598 (4)	−0.0118 (3)	0.46730 (22)	2.46 (13)
C(3B)	0.5057 (4)	−0.0227 (3)	0.36233 (24)	2.69 (13)
C(4B)	0.3746 (5)	0.0447 (3)	0.3026 (3)	3.44 (15)
C(5B)	0.3664 (5)	−0.0036 (4)	0.2060 (3)	4.51 (19)
C(6B)	0.4936 (5)	−0.0987 (4)	0.2023 (3)	4.58 (18)
C(7B)	0.5803 (5)	−0.1109 (3)	0.2965 (3)	3.44 (13)
C(8B)	0.6148 (8)	0.3399 (5)	0.0283 (4)	7.2 (3)
C(9B)	0.5431 (7)	0.2328 (4)	0.0750 (3)	5.34 (22)
C(10B)	0.6648 (5)	0.1943 (3)	0.1603 (3)	3.86 (16)
C(11B)	0.6716 (5)	0.2458 (3)	0.2563 (3)	3.98 (17)
C(12B)	0.8054 (6)	0.1363 (4)	0.3166 (3)	4.71 (19)
C(13B)	0.8842 (5)	0.0965 (4)	0.2254 (4)	5.32 (22)
C(14B)	0.7983 (6)	0.1025 (4)	0.1607 (3)	4.52 (19)
H(1A1)	0.380	0.721	0.437	4.5
H(1A2)	0.613	0.702	0.450	4.5
H(1A3)	0.497	0.709	0.552	2.6
H(4A)	0.172	0.350	0.406	4.1
H(5A)	0.065	0.335	0.215	4.6
H(6A)	0.232	0.511	0.134	4.6
H(7A)	0.442	0.636	0.274	4.2
H(8A1)	−0.021	0.581	0.035	11.3
H(8A2)	−0.186	0.687	−0.001	11.3
H(8A3)	−0.130	0.670	0.135	2.6
H(9A1)	0.109	0.764	0.135	9.5
H(9A2)	−0.105	0.826	0.140	9.5
H(11A)	−0.207	0.512	0.219	5.9
H(12A)	−0.144	0.496	0.409	6.7
H(13A)	0.091	0.673	0.479	6.0
H(14A)	0.167	0.797	0.330	6.5
H(1B1)	0.837	0.000	0.443	4.2
H(1B2)	0.783	−0.129	0.505	4.2
H(1B3)	0.796	0.016	0.564	2.6
H(4B)	0.318	0.132	0.327	4.4
H(4B)	0.303	0.042	0.142	5.6
H(6B)	0.544	−0.138	0.136	5.4
H(7B)	0.703	−0.158	0.314	4.5
H(8B1)	0.550	0.359	−0.036	2.6
H(8B2)	0.759	0.322	0.017	8.5
H(8B3)	0.621	0.421	0.078	8.5
H(9B1)	0.415	0.259	0.096	6.5
H(9B2)	0.523	0.156	0.211	6.5
H(11B)	0.567	0.302	0.283	5.0
H(12B)	0.820	0.190	0.397	5.8
H(13B)	0.967	0.021	0.283	6.1
H(14B)	0.805	0.030	0.102	5.7

[a] U_{iso} is the equivalent isotropic U defined as one-third of the trace of the orthogonalized U_{ij} tensor.

($CDCl_3$) δ 1.081 (t, 6 H, $-CH_3$), 2.108 (s, 5.9 H, $=CCH_3$), 2.240 (q, 4 H, $-CH_2$), 3.845 (d, 4 H, Cp H_β), 3.955 (d, 4 H, Cp H_α), 3.978 (s, 8 H, Cp $H_{\alpha,\beta}$); electron-impact mass spectrum M^+ at *m*/*e* 480.

The iodine oxidation compounds were all prepared in the same fashion. The parent biferrocene (50 mg, 0.1 mmol) was dissolved in 25 mL of benzene, and a solution of iodine (79 mg, 0.3 mmol) dissolved in benzene (25 mL) was added dropwise with rapid stirring. The resulting solid was filtered, washed with a little benzene, and vacuum-dried. See Table I for analyses.

Physical Measurements. ^1H NMR spectra were recorded on a Bruker MSL 200 spectrometer. Mass spectra were recorded on a Hewlett-Packard GC/MS system, Model 5995.

Polarographic measurements were carried out with a Princeton Applied Research Model 174 polarograph. Cyclic voltammetry was performed with a stationary Pt electrode, which was cleaned after each run. Duplicate runs were made on each sample. Various ferrocenes were studied in 1 × 10^{-3} M acetonitrile solutions with 0.1 M $(n\text{-}C_4H_9)_4NBF_4$ as supporting electrolyte. Degassing with nitrogen prefaced each run. The potentials quoted in this work are referred to a saturated aqueous calomel electrode at 25 °C.

Near-IR spectra were recorded with a Perkin-Elmer Lambda 9 spectrophotometer. The near-IR spectra were recorded from 2300 to 900 nm in CD_2Cl_2 by using 1.0-cm quartz cells. Owing to the small comproportionation constant, we were not able to isolate the pure mixed-valence complexes of **2** and **3** as salts. The mixed-valence solutions for **2** and **3** were generated by mixing equal concentrations of neutral and dioxidized complexes. Quantitative calculations based on the concentrations of mixed-valence complexes have been corrected from the comproportionation constant.

X-ray Structure Solution and Refinement for 2. A blocklike crystal (0.15 × 0.50 × 0.50 mm) of **2** grown by the CH_2Cl_2/hexane diffusion technique was used for data collection in the $\theta/2\theta$ scan mode at room temperature on an Enraf-Nonius CAD4 diffractometer at National Taiwan University. Details of data collection may be found in Table II. No evidence for crystal decomposition was noted. The cell constants, listed in Table II, were obtained by a least-squares fit to the automatically centered settings for 25 strong reflections. The data were corrected for absorption.

The structure of **2** was solved by the heavy-atom method. All non-hydrogen atoms were refined anisotropically. The final positional parameters for all atoms can be found in Table III, and the selected bond distances and angles can be found in Table IV.

Results and Discussion

The synthetic route to **2** and **3** was based on the work of Corey and co-workers, who produced a number of reagents for the intermolecular and intramolecular coupling of ketones and aldehydes.[11] Although the $TiCl_4$–$LiAlH_4$ reagent successfully couples ferrocenecarbaldehyde and acetylferrocene, it was found that only the complex with the *E* olefin linkage could be isolated.[12] However, we have found that two isomers, with *E* and *Z* linkages, respectively, could be isolated in the coupling of 1-ethyl-1′-acetylferrocene by $TiCl_4$–$LiAlH_4$. Possibly this is due to the ethyl substituent, which is designed in connection with our interest in discovering the influence of ligand structure in electron transfer as found in compounds **1b–e**.[6] Although the physical properties

---

(11) Corey, E. J.; Danhriser, R. L.; Chandrasekaran, S. *J. Org. Chem.* **1976**, *41*, 260.

(12) (a) Kashara, A.; Izumi, T. *Chem. Lett.* **1978**, 21. (b) Mukaiyama, T.; Sato, T.; Hanna, T. *Chem. Lett.* **1973**, 1041.

Table IV. Selected Bond Distances and Angles for **2**

Interatomic Distances, Å			
Fe(1A)–C(3A)	2.067 (3)	C(5A)–C(6A)	1.418 (6)
Fe(1A)–C(4A)	2.031 (3)	C(6A)–C(7A)	1.434 (5)
Fe(1A)–C(5A)	2.026 (4)	C(8A)–C(9A)	1.433 (11)
Fe(1A)–C(6A)	2.032 (4)	C(9A)–C(10A)	1.527 (9)
Fe(1A)–C(7A)	2.029 (3)	C(10A)–C(11A)	1.421 (7)
Fe(1A)–C(10A)	2.042 (4)	C(10A)–C(14A)	1.389 (7)
Fe(1A)–C(11A)	2.046 (4)	C(11A)–C(12A)	1.409 (7)
Fe(1A)–C(12A)	2.036 (4)	C(12A)–C(13A)	1.424 (7)
Fe(1A)–C(13A)	2.032 (4)	C(13A)–C(14A)	1.397 (8)
Fe(1A)–C(14A)	2.037 (4)	C(1B)–C(2B)	1.511 (5)
Fe(1B)–C(3B)	2.075 (3)	C(2B)–C(2B)	1.364 (6)
Fe(1B)–C(4B)	2.034 (4)	C(2B)–C(3B)	1.464 (5)
Fe(1B)–C(5B)	2.035 (4)	C(3B)–C(4B)	1.440 (5)
Fe(1B)–C(6B)	2.032 (4)	C(3B)–C(7B)	1.446 (5)
Fe(1B)–C(7B)	2.038 (4)	C(4B)–C(5B)	1.407 (6)
Fe(1B)–C(10B)	2.037 (4)	C(6B)–C(7B)	1.403 (6)
Fe(1B)–C(11B)	2.031 (4)	C(8B)–C(9B)	1.493 (7)
Fe(1B)–C(12B)	2.040 (4)	C(9B)–C(10B)	1.488 (6)
Fe(1B)–C(13B)	2.032 (4)	C(10B)–C(11B)	1.411 (6)
Fe(1B)–C(14B)	2.035 (4)	C(10B)–C(14B)	1.417 (6)
C(1A)–C(2A)	1.509 (5)	C(11B)–C(12B)	1.410 (6)
C(2A)–C(2A)	1.346 (6)	C(12B)–C(13B)	1.436 (7)
C(2A)–C(3A)	1.481 (5)	C(13B)–C(14B)	1.399 (7)
C(3A)–C(4A)	1.433 (5)	C(3A)–C(7A)	1.425 (5)
C(4A)–C(5A)	1.404 (5)		
Angles, deg			
C(1A)–C(2A)–C(2A)	122.8 (3)	C(1B)–C(2B)–C(3B)	114.8 (3)
C(1A)–C(2A)–C(3A)	114.2 (3)	C(2B)–C(2B)–C(3B)	122.4 (3)
C(2A)–C(2A)–C(3A)	123.0 (3)	C(2B)–C(3B)–C(4B)	130.4 (3)
C(2A)–C(3A)–C(4A)	129.9 (3)	C(2B)–C(3B)–C(7B)	124.0 (3)
C(2A)–C(3A)–C(7A)	123.9 (3)	C(4B)–C(3B)–C(7B)	105.6 (3)
C(4A)–C(3A)–C(7A)	106.2 (3)	C(3B)–C(4B)–C(5B)	108.8 (3)
C(3A)–C(4A)–C(5A)	109.3 (3)	C(4B)–C(5B)–C(6B)	108.3 (3)
C(4A)–C(5A)–C(6A)	108.4 (3)	C(5B)–C(6B)–C(7B)	108.4 (3)
C(5A)–C(6A)–C(7A)	107.1 (3)	C(3B)–C(7B)–C(6B)	108.8 (3)
C(3A)–C(7A)–C(6A)	108.9 (3)	C(8B)–C(9B)–C(10B)	112.8 (4)
C(8A)–C(9A)–C(10A)	113.5 (6)	C(9B)–C(10B)–C(11B)	125.9 (4)
C(9A)–C(10A)–C(11A)	131.7 (5)	C(9B)–C(10B)–C(14B)	127.1 (4)
C(9A)–C(10A)–C14A)	121.0 (5)	C(11B)–C(10B)–C(14B)	107.0 (4)
C(11A)–C(10A)–C(14A)	107.0 (4)	C(10B)–C(11B)–C(12B)	109.5 (4)
C(10A)–C(11A)–C(12A)	108.5 (4)	C(11B)–C(12B)–C(13B)	106.5 (4)
C(11A)–C(12A)–C(13A)	107.2 (4)	C(12B)–C(13B)–C(14B)	108.2 (4)
C(12A)–C(13A)–C(14A)	107.4 (4)	C(10B)–C(14B)–C(13B)	108.8 (4)
C(10A)–C(14A)–C(13A)	109.8 (4)	C(1B)–C(2B)–C(2B)	122.9 (3)

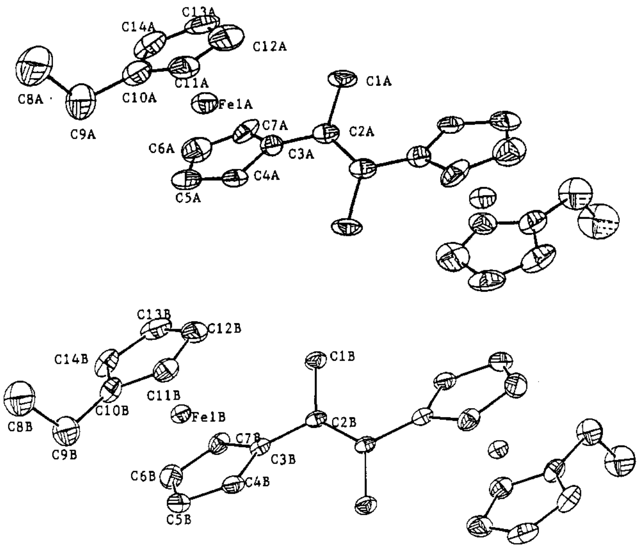

Figure 1. ORTEP plot of two crystallographically independent molecules of **2**. Hydrogen atoms are deleted for clarity.

of two isomers are different, for instance, NMR, it is difficult to assign their structures with certainty. It appears that only single-crystal X-ray crystallography can be applied. Unfortunately, a suitable single crystal of the *Z* isomer could not be obtained. Before the new physical data are described, a summary of single-crystal X-ray structural results obtained for the *E* isomer will be presented.

Molecular Structure of 2. The results of our crystallographic study of **2** show that it crystallizes in the triclinic space group $P\bar{1}$. As required by the presence of the center of symmetry, the molecule assumes a trans conformation with two ferrocenyl units on opposite sides of ethenyl bridge plane. There are two crystallographically independent molecules in the unit cell, and the molecular structures are shown in Figure 1. There is a very similar geometrical arrangement in the two independent molecules. The cyclopentadienyl rings associated with Fe(1A) and Fe(1B) are rotated 37.9 and 37.4°, respectively, from a conformation that would place them perpendicular to the ethylene best plane. The dihedral angles between the two five-membered rings of the $\mathrm{Fe_{1A}(\eta^5\text{-}C_5H_4)(\eta^5\text{-}C_5H_4)}$ and $\mathrm{Fe_{1B}(\eta^5\text{-}C_5H_4)(\eta^5\text{-}C_5H_4)}$ moieties are 1.22 and 2.34°, respectively. Furthermore, the two rings of the $\mathrm{Fe_{1A}(\eta^5\text{-}C_5H_4)(\eta^5\text{-}C_5H_4)}$ and $\mathrm{Fe_{1B}(\eta^5\text{-}C_5H_4)(\eta^5\text{-}C_5H_4)}$ moieties are nearly eclisped with an average staggered angle of 10.11 and 2.19°, respectively. The average bond distance (2.038 (4) Å) between the Fe atoms and the five carbon atoms of a given ring is close to the 2.045-Å distance observed for ferrocene.[13] The centroid-to-centroid distances between the two rings associated with atoms Fe(1A) and Fe(1B) are 3.26 and 3.29 Å, respectively. The average of these two values is also close to the 3.30-Å distance observed for ferrocene. The average C–C bond length in the rings agrees well with that in ferrocene. The C–C bond distances in the two crystallographically independent ethyl substituents are 1.493 (7) and 1.433 (11) Å. The average bond length is 1.463 (9) Å, which is shorter than the 1.50-Å length found in 1′,1‴-diethylbiferrocene.[14] Librational motion will cause an apparent shortening of the C–C bonds, and the magnitude of this effect will be greater in **2** if there is less intra- and intermolecular constraint.

Table V. Polarographic Data for Various Biferrocenes

compound	$E_{1/2}$,[a] V		Δ,[b] mV	$\Delta E_{1/2}$,[c] V	K_{com}[d]
	cyclic volt	diff pulse			
ferrocene	0.400	0.400	65		
biferrocene	0.31	0.300	70	0.31	1.80×10^5
	0.62	0.610	75		
2	0.330	0.330	75	0.15	3.49×10^2
	0.475	0.465	80		
3	0.325	0.330	75	0.15	3.49×10^2
	0.475	0.480	80		

[a] All half-wave potentials are referred to the SCE, employing a stationary Pt electrode (sweep rate 200 mV/s for CV and 2 mV/s for DP). [b] Peak-to-peak separation between the resolved reduction and oxidation wave maxima. [c] Peak separation between two waves. [d] Comproportionation constant.

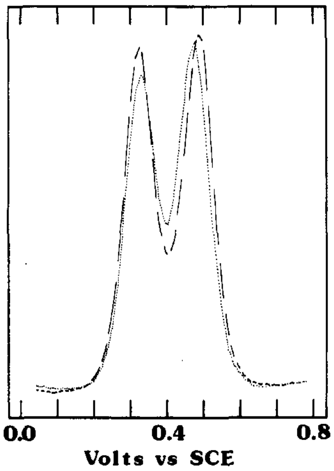

Figure 2. Differential pulsed polarogram for **2** (dotted curve) and **3** (dashed curve).

Electrochemical Results. The polarographic data for compounds **2** and **3** are shown in Table V. It is a dilemma that the electrochemical results show no significant difference between **2** and **3** (Figure 2). The $E_{1/2}$ values for the two waves of **2** and **3** are 0.33 and 0.48 V. A comparison of the magnitudes of peak-to-peak

---

(13) Seiler, P.; Dunitz, J. D. *Acta Crystallogr., Sect. B* **1979**, *35*, 1068.

(14) Kaluski, Z. L.; Struchkov, Yu. T. *Zh. Strukt. Khim.* **1965**, *6*, 104.

Table VI. Near-IR Band Maxima for Mixed-Valence Compounds in CD_2Cl_2 at 25 °C

complex	λ_{max}, nm	ϵ, M^{-1} cm^{-1}	$\Delta\nu_{1/2}$,[a] cm^{-1} obsd	$\Delta\nu_{1/2}$,[a] cm^{-1} calcd
1a	2200	980	3670	3240
mixed-valence cation of **2**	2000	650	4600	3400
mixed-valence cation of **3**	2000	650	4600	3400

[a] Half-width from the equation[12] $\Delta\nu_{1/2}$ (cm^{-1}) = $(2300\lambda_{max})^{1/2}$.

separations ($\Delta E_{1/2}$) of **2** and **3** with that of biferrocene indicates that the interaction between the two Fe sites is smaller in **2** and **3**. In the bridged biferrocenes there are two possible types of interaction between the two ferrocene moieties: interaction propagated through the bridge and through space (electric field effect). It is reasonable to believe that the interaction through the bridge between two Fe sites is strongly favored. Therefore, we observed a decrease in interaction with an increase of Fe–Fe distance. *E–Z* and *Z–E* isomerizations are proposed to explain the similarity of electrochemical data between **2** and **3**, and they will be discussed in more detail in the last section.

Coulometry experiments showed that each of the two waves is a one-electron-transfer process. In eq 1 the abbreviation [3,3]

$$[3,3] + [2,2] \rightleftharpoons 2[2,3] \tag{1}$$

is for the dioxidized salt, [2,3] for the monooxidized salts, and [2,2] for the neutral compound. *K* for this comproportionation equilibrium is 349, as calculated from the $E_{1/2}$ values at 25 °C. Quantitative calculations based on [2,3], which appear later in this paper, have been corrected for the equilibrium.

Near-Infrared Spectra. In common with most mixed-valence complexes, the mixed-valence complexes of **2** and **3** each have a near-IR transition at 2000 nm, which is not present for the neutral complex or dioxidized ion. The band is very weak ($\epsilon = 650$ M^{-1} cm^{-1} in CD_2Cl_2; Table VI) and is 35% broader than what is expected on the basis of the equation given by Hush[15] ($\Delta\nu_{1/2} = 4.60 \times 10^3$ cm^{-1} compared to a calculated value of 3.40×10^3 cm^{-1}). An agreement, to about 10%, between $\Delta\nu_{1/2cal}$ and $\Delta\nu_{1/2obs}$ is usually taken as an indication that the Hush model is a satisfactory description of a mixed-valence system. In the case of **1a**, a good agreement is observed.

The appearance of a broader IT band in the mixed-valence cation of **2** or **3** could occur because of the isomerization in the mixed-valence cations. In other words, it could conceivably mean that more than one IT band exists. The *E–Z* and *Z–E* isomerizations in the mixed-valence cations are evident by NMR studies. The solutions, which are obtained by chemical reduction of the dioxidized cations and the "mixed-valence solutions" with $Na_2S_2O_3$, do show both *E* and *Z* isomers (≈35% *Z* isomer and ≈65% *E* isomer). It should be mentioned that the isomerization is not observed in a solution of neutral complex, **2** or **3**. It is possible that the isomerizations are associated with thermal electron transfer or photoinduced electron transfer through the π^* orbital of ethene bridge in mixed-valence [2,3]. It is also possible that the isomerizations are through the dioxidized cations, since the mixed-valence solutions contain ≈5% dioxidized cations. The C–C bond order of ethene bridge in dication [3,3] is decreased by means of conjugation between the ethene unit and the two ferrocenium moieties. In mixed-valence compounds it is possible to estimate the rate of electron transfer from the IT band absorption data.[3b] Owing to the isomerization, the thermal energy of activation and the rate of electron transfer calculated in this way will be rough estimates.

Recently, the contribution of the bridge in bridged mixed-valence dimers to the line shape of the IT band has captured considerable attention.[16] In those studies, a three-site model for bridged mixed-valence dimers is proposed. From this model, one can calculate the contribution of the bridge to the absorption profile of the IT band. In this model, one considers the degree of the delocalization for the unpaired electron in the bridge. It is possible that the delocalization of the unpaired electron in the π^* orbital of the ethene bridge in the mixed-valence cations of **2** and **3** causes the isomerizations.

Acknowledgment. We are grateful for support from the ROC National Science Council (Grant NSC-77-0208-M001-01).

Registry No. **1a**, 39470-17-2; **2**, 120172-58-9; **2**(I_3), 120172-60-3; **3**, 120292-75-3; **3**(I_3), 120292-77-5; $TiCl_4$, 7550-45-0; 1-ethyl-1′-acetylferrocene, 1316-96-7; biferrocene, 1287-38-3.

Supplementary Material Available: Listings of experimental and crystal data and anisotropic thermal parameters (3 pages); a table of observed and calculated structure factors (26 pages). Ordering information is given on any current masthead page.

---

(15) Hush, N. S. *Prog. Inorg. Chem.* **1967**, *8*, 391.

(16) (a) Root, L. J.; Ondrechen, M. J. *Chem. Phys. Lett.* **1982**, *93*, 421. (b) Ondrechen, M. J.; Ko, J.; Root, L. J. *J. Phys. Chem.* **1984**, *88*, 5919. (c) Ko, J.; Ondrechen, M. J. *Chem. Phys. Lett.* **1984**, *112*, 507. (d) Wong, K. Y. *Chem. Phys. Lett.* **1986**, *125*, 485.